www.ceramsoc.com/en/
CrossMark
Available online at www.sciencedirect.com
ScienceDirect
J Materiomics 2 (2016) 324–330
www.journals.elsevier.com/journal-of-materiomics/

Effect of Cd isoelectronic substitution on thermoelectric properties of $Zn_{0.995}Na_{0.005}Sb$

Jingchao Zhou [a], Lihong Huang [b], Zhengyun Wang [b], Zihang Liu [a], Wei Cai [a], Jiehe Sui [a,*]

[a] National Key Laboratory Precision Hot Processing of Metals, School of Materials Science and Engineering, Harbin Institute of Technology, Harbin 150001, China

[b] Center for Advanced Materials and Energy, Xihua University, Chengdu, Sichuan 610039, China

Received 24 March 2016; revised 28 August 2016; accepted 29 August 2016
Available online 6 September 2016

Abstract

ZnSb as a kind of material with abundant resource and low cost has a low thermal conductivity and a high Seebeck coefficient, giving the potential of high thermoelectric properties. In this paper, Cd isoelectronic substitution was adopted to further improve the thermoelectric performance by reducing the lattice thermal conductivity of ZnSb. The results show that Cd substitution reduces the lattice thermal conductivity and increases the electrical conductivity. A high *ZT* value of 1.22 is achieved at 350 °C for $Zn_{0.915}Na_{0.005}Cd_{0.08}Sb$.

Keywords: ZnSb; Isoelectronic substitution; Lattice thermal conductivity; Thermoelectric properties

1. Introduction

Thermoelectric (TE) material is known as a promising kind of new energy material. The reuse of waste heat has attracted much recent attention. For the middle-temperature field, the most widely used TE material is PbTe [1–4]. However, Pb is toxic, and Te is scarce and expensive. ZnSb based TE materials have been developed due to the abundant resource and relatively high conversion efficiency since the discovery of the Seebeck effect [5–12].

The performance of TE material is usually determined by the dimensionless figure of merit, $ZT = (\sigma S^2/\kappa)T$, where S, σ, κ and T are the Seebeck coefficient, electrical conductivity, thermal conductivity and absolute temperature, respectively. It is well known that the electronic (S, σ) and thermal (κ) transport properties are interdependent, changing one will negatively affect the others. Therefore, improving the *ZT* value has become a challenge [13–20].

ZnSb is a p-type semiconductor with a *Pbca* space group, an orthorhombic crystal structure and a band gap of about 0.2 eV. According to phase diagram, there is no phase transformation from room temperature to the melting temperature of 819 K. ZnSb is much more stable than other kinds of Zn–Sb compounds such as Zn_4Sb_3 [7]. Much effort had been made to improve the thermoelectric performance of ZnSb. For instance, a mechanical grinding method was applied to reduce the thermal conductivity, and the *ZT* value was increased from 0.2 to 0.9 at 550 K [8]. The maximum *ZT* value of 1 at 630 K was obtained by Sn acceptor doping and Cd isoelectronic substitution in the ZnSb system [21]. ZnSb with 0.2% Ag doping had a *ZT* value as high as 1.15, but Ag doping caused the massive cracks [22].

Recently, Na as an acceptor doping improves the electrical conductivity and power factor and reduces the lattice thermal conductivity. The *ZT* value of 1 at 350 °C is obtained for the optimal composition $Zn_{0.995}Na_{0.05}Sb$ [23]. However, the lattice thermal conductivity is relatively high (i.e., ~1.75 W/m·K

* Corresponding author.
E-mail address: suijiehe@hit.edu.cn (J. Sui).
Peer review under responsibility of The Chinese Ceramic Society.

http://dx.doi.org/10.1016/j.jmat.2016.08.003

at room temperature). Isoelectronic substitution is an effective way to reduce the lattice thermal conductivity, thereby leading to improve the *ZT* value, which has been confirmed in the thermoelectric materials, such as Half-Heusler, GeSi, Bi_2Te_3 [24–26]. In the case of ZnSb, Zn and Cd belong to the same column, and Cd has a greater ionic radius and a heavier atomic mass, compared to Zn. Therefore, an enhanced *ZT* value is expected due to the reduced lattice thermal conductivity caused by the size and mass fluctuation between Cd and Zn. In this paper, the effect of Cd isoelectronic substitution on the thermoelectric properties of $Zn_{0.995}Na_{0.005}Sb$ is investigated.

2. Experimental

Na (99.99%), Zn (99.99%), Cd (99.99%), and Sb (99.99%) were weighted and sealed in evacuated quartz tubes according to the formula of $Zn_{0.995-x}Na_{0.005}Cd_xSb$ (x = 0, 0.04, 0.08, 0.12). The quartz tubes were heated at 923 K for 10 h, and then quenched in cold water. The powder was obtained after ball milling for 2 h. The obtained powder was hot pressed at a sintering temperature of 673 K for 2 min under a pressure of 60 MPa.

The crystal structures of $Zn_{0.995-x}Na_{0.005}Cd_xSb$ were characterized by X-Ray diffraction (XRD) and the lattice parameters were calculated by peak fitting using the JADE 5.0 program. The grain size was determined by scanning electron microscopy (SEM).

The electrical resistivity and the Seebeck coefficient were measured by ZEM-3 (UlvacRiko ZEM-3) in Ar atmosphere. The hall coefficient (R_H) was measured by a four probe method. The carrier concentration (n) and mobility (μ) at room temperature were calculated by the equations of $n = 1/eR_H$ and $\mu = \sigma R_H$. The thermal diffusivity (D) was measured on a laser flash apparatus (Netzsch LFS 457) with flowing argon gas protection. The specific heat capacity (C_p) was calculated by using the Dulong-Petit law of $C_v = 3NR/M$, where N is the number of atoms per molecule, $R = 8.314$ J mol^{-1} K^{-1} and M is the atomic mass per molecule. The densities (ρ) of all samples were measured by an Archimedes method, and the relative densities of all samples are greater than 96%. The thermal conductivity (κ) was calculated using the equation of $\kappa = D \cdot \rho \cdot C_p$.

3. Results and discussion

Fig. 1 shows the powder XRD patterns of the $Zn_{0.995-x}Na_{0.005}Cd_xSb$ (x = 0, 0.04, 0.08 and 0.12). All the major Bragg peaks show an excellent match to the simulated pattern of ZnSb (PDF#37-1008) and can be indexed as the *Pbca* space group. No obvious impurity phase appears within the detectability limit of XRD. The peaks of XRD patterns slightly shift to the lower diffraction angle when the Cd content increases. Correspondingly, the lattice parameters of the samples are calculated and listed in Table 1. Clearly, Cd substitution increases the lattice parameters due to the difference of ionic radius between Cd^{2+} (0.95 Å) and Zn^{2+} (0.74 Å). Therefore, it can be concluded that the Cd is incorporated into the lattice in $Zn_{0.995-x}Na_{0.005}Cd_xSb$.

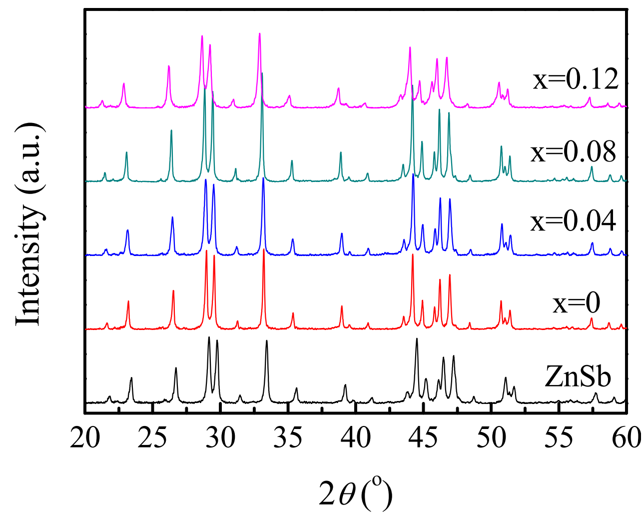

Fig. 1. Powder XRD patterns of ZnSb and $Zn_{0.995-x}Na_{0.005}Cd_xSb$ (x = 0, 0.04, 0.08 and 0.12).

Table 1
Lattice parameters of ZnSb and $Zn_{0.995-x}Na_{0.005}Cd_xSb$ samples.

Sample	*a* (Å)	*b* (Å)	*c* (Å)
ZnSb	6.205	7.737	8.085
$Zn_{0.995}Na_{0.005}Sb$	6.208	7.743	8.095
$Zn_{0.955}Na_{0.005}Cd_{0.04}Sb$	6.216	7.756	8.101
$Zn_{0.915}Na_{0.005}Cd_{0.08}Sb$	6.218	7.759	8.105
$Zn_{0.875}Na_{0.005}Cd_{0.12}Sb$	6.223	7.766	8.110

Table 2 shows the room temperature carrier concentration and mobility. As ZnSb is a kind of p-type semiconductor, a small amount of Na acceptor doping can result in a significant increase in the carrier concentration. From Table 2, the carrier concentration increases when the Cd substitution content increases to 8%. However, the carrier concentration decreases obviously when the Cd substitution content increases to 12%. The mechanism for the enhancement of carrier concentration due to the Cd substitution is unclear until now. The carrier mobility decreases with the increase of the Cd substitution content due to the increased defect scattering. In addition, the change of both carrier concentration and carrier mobility as a function of Cd content can further confirm that Cd is incorporated into the lattice in $Zn_{0.995-x}Na_{0.005}Cd_xSb$.

Fig. 2 shows the fracture morphologies of $Zn_{0.995-x}Na_{0.005}Cd_xSb$. The grain size ranges from 0.8 μm to 1.2 μm for all the samples. This indicates that Cd substitution has no obvious influence on the grain size. The grain size is

Table 2
Room temperature carrier concentration and mobility as a function of Cd doping for $Zn_{0.995-x}Na_{0.005}Cd_xSb$.

Sample	Carrier concentration (cm^{-3})	Carrier mobility (cm^2/Vs)
$Zn_{0.995}Na_{0.005}Sb$	6.12×10^{18}	289.9
$Zn_{0.955}Na_{0.005}Cd_{0.04}Sb$	8.69×10^{18}	288.4
$Zn_{0.915}Na_{0.005}Cd_{0.08}Sb$	10.07×10^{18}	262.5
$Zn_{0.875}Na_{0.005}Cd_{0.12}Sb$	6.15×10^{18}	209.3

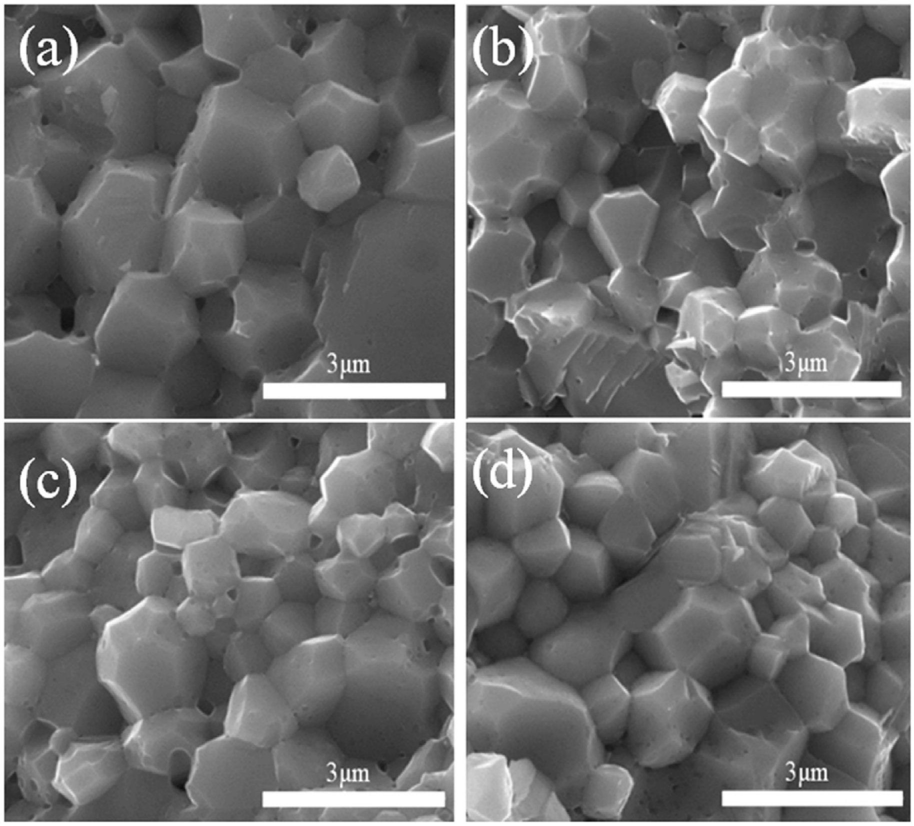

Fig. 2. Fracture morphologies of $Zn_{0.995-x}Na_{0.005}Cd_xSb$ (a) x = 0, (b) x = 0.04, (c) x = 0.08, (d) x = 0.12.

obtained after ball milling for 2 h and hot press. It is expected that the grain size can be further reduced by prolonging ball milling time, thereby leading to the decrease of the lattice thermal conductivity.

Fig. 3 shows the temperature dependence of electrical properties for $Zn_{0.995-x}Na_{0.005}Cd_xSb$ samples. In Fig. 3(a), the electrical resistivity firstly decreases from 2.63×10^{-5} Ω m as x = 0 to 2.07×10^{-5} Ω m as x = 0.08 at room temperature, and then increases to 3.55×10^{-5} Ω m as x = 0.12 with increasing the Cd content, which is similar to the change tendency of carrier concentration. Considering that the carrier mobility decreases with the increase of Cd substitution, we find that the increased electrical conductivity of $Zn_{0.995-x}Na_{0.005}Cd_xSb$ is mostly due to the increased carrier concentration, according to the equation of $\sigma = ne\mu$.

In Fig. 3(b), the positive Seebeck coefficients indicate p-type semiconductor for ZnSb-based materials. Similarly, the Seebeck coefficients at room temperature first decrease and then increase with increasing the Cd content, consistent with the tendency of electrical resistivity. All the samples exhibit the peak values of the Seebeck coefficient at 350 °C, showing the typical characteristic of bipolar diffusion effect.

Fig. 3(c) shows the power factor ($PF = \sigma S^2$) calculated from the measured electrical resistivity and Seebeck coefficient. The power factor of $Zn_{0.995-x}Na_{0.005}Cd_xSb$ samples (as x = 0.04 and 0.08) increases in the whole measured temperature range due to the decreased electrical resistivity. The maximum power factor reaches 20.6 μW/cm·K^2 for $Zn_{0.915}Na_{0.005}Cd_{0.08}Sb$ at 200 °C, which is greater than that of the sample without Cd substitution (i.e., ~18.5 μW/cm·K^2 at 200 °C).

Fig. 4(b) shows the total thermal conductivity (κ_{tot}) as a function of temperature for $Zn_{0.995-x}Na_{0.005}Cd_xSb$ samples, which is calculated by the thermal diffusivity shown in Fig. 4(a) and the density shown in Table 3. Normally, the κ_{tot} consists of three parts, i.e., lattice thermal conductivity (κ_{lat}), electronic thermal conductivity (κ_{ele}), and bipolar thermal conductivity (κ_{bip}). κ_{ele} can be easily estimated from the Wiedemann−Franz relationship ($\kappa_{ele} = L\sigma T$), where L is the Lorenz number, as shown in Fig. 4(c). The Lorenz number is obtained by fitting the respective Seebeck coefficient values with an estimate of the reduced chemical potential using a single parabolic band (SPB) model (Eqs. (1)−(3)) [27], where k_B is the Boltzmann constant, h is the Plank constant, e is the electron charge, $F_n(\eta)$ is the nth order Femi integral, η is the reduced Fermi energy, χ is the variable of integration, rather than using a constant value of 2.45×10^{-8} W Ω K^{-2} for degenerate semiconductor.

$$L = \left(\frac{k_B}{e}\right)^2 \left[\frac{3F_2(\eta)}{F_0(\eta)} - \left(\frac{2F_1(\eta)}{F_0(\eta)}\right)^2\right] \tag{1}$$

$$S = \pm\frac{k_B}{e}\left(\frac{2F_1(\eta)}{F_0(\eta)} - \eta\right) \tag{2}$$

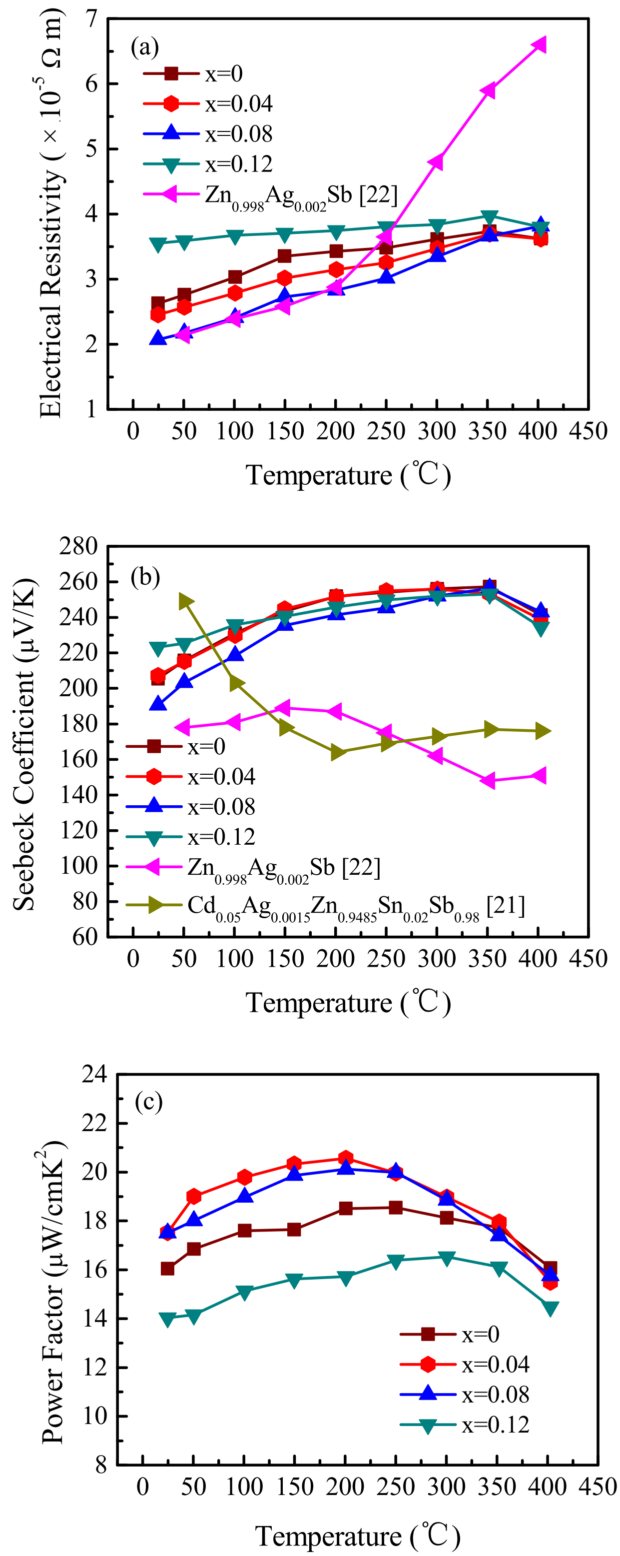

Fig. 3. Electrical transport properties of $Zn_{0.995-x}Na_{0.005}Cd_xSb$ (a) Electrical resistivity, (b) Seebeck coefficient and (c) Power factor.

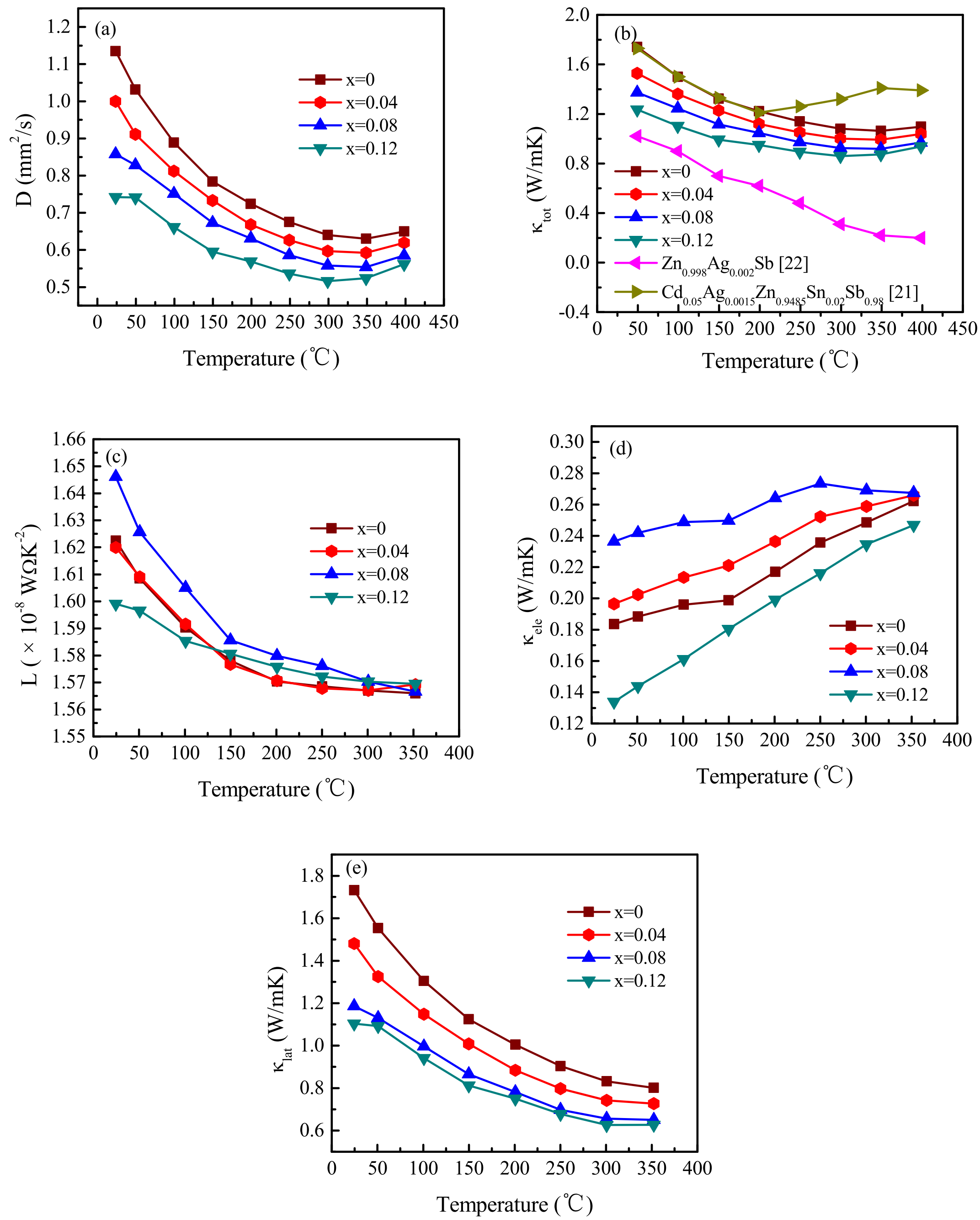

Fig. 4. Thermal transport properties of $Zn_{0.995-x}Na_{0.005}Cd_xSb$ (a) Thermal diffusivity, (b) Total thermal conductivity, (c) Lorenz number, (d) Electronic thermal conductivity, (e) Lattice thermal conductivity.

Table 3
Sample density for $Zn_{0.995-x}Na_{0.005}Cd_xSb$.

Sample	Density (g/cm^3)
$Zn_{0.995}Na_{0.005}Sb$	6.328
$Zn_{0.955}Na_{0.005}Cd_{0.04}Sb$	6.334
$Zn_{0.915}Na_{0.005}Cd_{0.08}Sb$	6.339
$Zn_{0.875}Na_{0.005}Cd_{0.12}Sb$	6.440

$$F_n(\eta) = \int_0^\infty \frac{x^n}{1+e^{x-\eta}}dx \quad (3)$$

In general, κ_{lat} can be estimated by directly subtracting κ_{ele} from κ_{tot}. In this case, because of the intrinsic excitation occurred at a high temperature, κ_{ele} and κ_{lat} are only calculated before the onset of bipolar effect, as shown in Fig. 4(d) and (e). It is easy to find that the total thermal conductivity decreases with the increase of the Cd content. The κ_{ele} has a similar tendency with the change of electrical resistivity caused by Cd substitution, as shown in Fig. 3(a). The κ_{lat} decreases from 1.73 W/m·K for $Zn_{0.995}Na_{0.005}Sb$ to 1.1 W/m·K for $Zn_{0.875}Na_{0.005}Cd_{0.12}Sb$ at room temperature with increasing the Cd content. The low thermal conductivity can be attributed to the strain fluctuation caused by the mass and

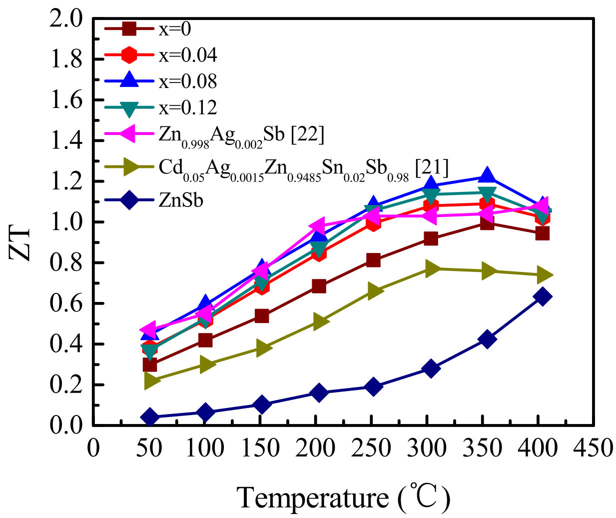

Fig. 5. *ZT* values of ZnSb and $Zn_{0.995-x}Na_{0.005}Cd_xSb$.

size fluctuation between Zn^{2+} (i.e., 65.38, 0.74 Å) and Cd^{2+} (i.e., 112.41, 0.95 Å).

Fig. 5 shows the *ZT* value calculated based on the electrical and thermal transport properties. The maximum *ZT* value is 1.22 at 350 °C for $Zn_{0.915}Na_{0.005}Cd_{0.08}Sb$ sample, which is greater than that of 0.99 for $Zn_{0.995}Na_{0.005}Sb$ sample and 0.45 for ZnSb sample. The present *ZT* value of 1.22 is greater than that of other ZnSb based thermoelectric materials [17−19]. The improved *ZT* value can be attributed to the enhanced power factor caused by the enhanced electrical conductivity, as shown in Fig. 3, and the reduced thermal conductivity, as shown in Fig. 4. In addition, the average *ZT* value is improved from 0.7 of the $Zn_{0.995}Na_{0.005}Sb$ sample to 0.912 of the $Zn_{0.915}Na_{0.005}Cd_{0.08}Sb$ sample due to the Cd substitution.

4. Conclusions

The effect of Cd isoelectric substitution for Zn in $Na_{0.005}Cd_{0.08}Sb$ on the thermoelectric properties was investigated. The $Zn_{0.915}Na_{0.005}Cd_{0.08}Sb$ showed a significant enhancement of *ZT* value from 0.45 for ZnSb to 1.22 at 350 °C, which could be ascribed to the enhanced power factor and the reduced thermal conductivity caused by the Cd substitution.

Acknowledgment

This work was supported by the National Natural Science Foundation of China (Nos. 51622101, 51471061 and 51271069).

References

[1] Pei Y, LaLonde A, Lwanaga S, Snyder GJ. High thermoelectric figure of merit in heavy hole dominated PbTe. Energy Environ Sci 2011;4:2085−9.
[2] Jaworski CM, Nielsen MD, Wang H, Girard SN, Cai W, Porter WD, et al. Valence-band structure of highly efficient p-type thermoelectric PbTe-PbS alloys. Phys Rev B 2013;87:4−15.
[3] Girard SN, He J, Xhou X, Shoemaker DP, Jaworski CM, Uher C, et al. High performance Na-doped PbTe−PbS thermoelectric materials: electronic density of states modification and shape-controlled nanostructures. J Am Chem Soc 2011;133:16588−97.
[4] He J, Zhao LD, Zheng JC, Doak JW, Wu H, Wang HQ, et al. Role of sodium doping in lead chalcogenide thermoelectrics. J Am Chem Soc 2013;135(12):4624−7.
[5] Zhang LT, Tsutsui M, Ito K. Effects of ZnSb and Zn inclusions on the thermoelectric properties of beta-Zn_4Sb_3. J Alloy Compd 2003;358(1):252−6.
[6] Arushanov EK. Crystal-growth, characterization and application of II-V compounds. Prog Cryst Growth Charact 1986;13:1−38.
[7] Shaver PJ, Blair J. Thermal and electronic transport properties of p-type ZnSb. J Phys Rev 1966;141(2):649.
[8] Okamura C, Ueda T, Hasezaki K. Preparation of single-phase ZnSb thermoelectric materials using a mechanical grinding process. Mater Trans 2010;51(5):860−2.
[9] Chung DY, Iordanidis L, Choi KS, Kanatzidis MG. Complex chalcogenides as thermoelectric materials: a solid state chemistry approach. Korean Chem Soc 1998;19:1283−93.
[10] Li W, Chen Z, Lin S, Chang Y, Ge B, Chen Y, et al. Band and scattering tuning for high performance thermoelectric $Sn_{1-x}Mn_xTe$ alloys. J Materiomics 2015;1(4):307−15.
[11] Sussardi A, Tanaka T, Khan AU, Schlapbach L, Mori T. Enhanced thermoelectric properties of samarium boride. J Materiomics 2015;1(3):196−204.
[12] Zhang X, Zhao LD. Thermoelectric materials: energy conversion between heat and electricity. J Materiomics 2015;1(2):92−105.
[13] Tang Y, Chen S, Snyder GJ. Temperature dependent solubility of Yb in Yb-$CoSb_3$ skutterudite and its effect on preparation, optimization and lifetime of thermoelectrics. J Materiomics 2015;1(1):75−84.
[14] DiSalvo FJ. Thermoelectric cooling and power generation. Science 1999;285(5428):703−6.
[15] Rowe DM. CRC handbook of Thermoelectrics. Voca Raton, FL: CTC; 1995.
[16] Rowe DM. Thermoelectric HandbookL macro to nano. Voca Raton, FL: CRC/Taylor and Francis; 2006.
[17] Wood C. Materials for thermoelectric energy conversion. Rep Prog Phys 1988;51(4):459.
[18] Sales BC, Mandrus D, Williams RK. Filled skutterudite antimonides: a new class of thermoelectric materials. Science 1996;272(5266):1325−8.
[19] Rowe DM. Thermoelectrics, an environmentally-friendly source of electrical power. Renew energy 1999;16(1):1251−6.
[20] Tritt TM, Subramanian MA. Thermoelectric materials, phenomena, and applications: a Bird's eye view. Mater Res Soc Bull 2006;31:188.
[21] Fedorov MI, Prokofeva LV, Pshenay-Severin DA, Shabaldin AA, Konstantinov PP. New interest in intermetallic compound ZnSb. J Electron Mater 2014;43:2314.
[22] Xiong DB, Okamoto NL, Inui H. Enhanced thermoelectric figure of merit in p-type Ag-doped ZnSb nanostructured with Ag_3Sb. Scr Mate 2013;69(5):397−400.
[23] Zihang Liu, Xianfu Meng, Jiehe Sui. NA doping for higher thermoelectric performance in P-type ZnSb. [Submitted to J Mater Sci Technol].
[24] Chai YW, Oniki T, Kenjo T, Kimura Y. The effect of an isoelectronic Ti-Zr substitution on Heusler nanoprecipitation and the thermoelectric properties of a ($Ti_{0.2}$, $Zr_{0.8}$)$Ni_{1.1}Sn$ half-Heusler alloy. J Alloy Compd 2016;662:566−77.
[25] Bouanani HG, Eddike D, Liautard B, Brun G. Solid state demixing in Bi_2Se_3-Bi_2Te_3 and Bi_2Se_3-In_2Se_3 phase diagrams. Mater Res Bull 1996;31(2):177−87.
[26] Nambuddee M, Moontragoon P. Calculation of electronic structure and thermoelectric properties of $Ge_{(1-x)}Si_x$ alloy. Chiang Mai J Sci 2013;40(6):1013−9.
[27] Zhao LD, Lo SH, He JQ. High performance thermoelectrics from earth-abundant materials: enhanced figure of merit in PbS by second phase nanostructures. J Am Chem Soc 2011;133(50):20476−87.

Jingchao Zhou is a Ph.D. candidate in the School of Materials Science and Engineering from Harbin Institute of Technology, China. He received his master's degree in the Department of Materials Physics and Chemistry from Harbin Institute of Technology. His research focuses on synthesis and characterization of nanostructured thermoelectric materials.

Dr. Lihong Huang is currently a research faculty in the Center for Advanced Materials and Energy at Xihua University of China, and also was a visiting scholar in the Department of Physics and TcSUH at the University of Houston. She obtained her Ph.D. degree in Materials Science from Sichuan University in 2012. Her current research interesting covers the fabrication, characterization of nanostructured thermoelectric materials, especially half-Heuslers.

Zhengyun Wang is currently a researcher in the Center for Advanced Materials and Energy, Xihua University, China. His current research is mainly on synthesis and characterization of phase change functional materials.

Zihang Liu is currently a Ph.D. candidate in the Department of Material Physics and Chemistry at Harbin Institute of Technology, China. He received his Bachelor degree from Material Science and Engineering at Inner Mongolia University of Technology. His current research is mainly on nanostructured thermoelectric materials and devices.

Dr. Wei Cai is currently a Professor and Head of the Material Physics and Chemistry at Harbin Institute of Technology. He obtained his Ph.D. degree from Harbin Institute of Technology in 1994. His research interests focus mainly on shape memory materials, nanomaterials and thermoelectric materials.

Dr. Jiehe Sui is currently a Professor of the Material Physics and Chemistry at Harbin Institute of Technology. He received his Ph.D. degree in the Department of Materials Physics and Chemistry from Harbin Institute of Technology, China. His current research is mainly on thermoelectric materials and devices.